Chemistry Research Journal, 2018, 3(3):179-185

Available online www.chemrj.org

Research Article

ISSN: 2455-8990
CODEN(USA): CRJHA5

Optical absorption improvement of PANI/$MnFe_2O_4$/ZnO photocatalyst under visible light irradiation

Nahid Rasouli*, Somayea Abasian

*Department of Chemistry, Payame Noor University, P.O. Box 19395-3697, Tehran, Iran

Abstract ZnO as a promising photocatalyst has gained main attention for degradation of organic pollutants from water environments. However, the main drawback of ZnO is the relatively lowphotocatalytic activity, because of high recombination rate of photoexcited electron-hole pairs that restrict its potential applications. Herein, novel magnetic photocatalyst of PANI/$MnFe_2O_4$/ZnO was synthesized by in situ oxidative polymerization of aniline in the presence of $MnFe_2O_4$ as magnetic component and ZnO as photoactive component. The physicochemical properties of synthesized sample was characterized by using X-ray diffraction (XRD), Fourier transform infrared spectroscopy (FT-IR), field emission scanning electron microscopy (FE-SEM) and UV–vis spectroscopy. The catalytic activity of the as prepared PANI/$MnFe_2O_4$/ZnO as photocatalyst was investigated by degradation of methyl orange (MO) as a model contaminant in aqueous solution under visible light irradiation. The obtained results indicated that the as prepared PANI/$MnFe_2O_4$/ZnO show highly enhanced photocatalytic activity for degradation of MOas compared with the parent materials, because of thesynergistic effect among ZnO, $MnFe_2O_4$ and PANI. Moreover, the magnetic photocatalyst of PANI/$MnFe_2O_4$/ZnO can be easily separated from the aqueous solution by an external magnet and reused for several cycles.

Keywords Polyaniline; Magnetically separable;visible light; Photocatalyst; ZnO

1. Introduction

Azo dyes used in textile and food industries are their important sources of the environmental contaminations due to their non-biodegradability and high toxicity and carcinogenic effects on humans [1, 2]. One of this class of dyes, Methyl Orange (MO)is a water-soluble azo dye (Fig. 1), widely used in the textile, printing, paper manufacturing, pharmaceutical and food industries and metabolizes into aromatic amines by intestinal microorganisms which can enters the body through ingestion and make intestinal cancer. Semiconductor research has demonstrated the main application in areas such as hydrogen production through photocatalytic water splitting [3, 4], dye sensitized solar cells [5] and photocatalytic treatment of harmful organics from air and water [6]. Among these investigations, developing of efficient visible light responsive photocatalysts for environmental remediation has become the main area in photocatalysis research because of the usage of solar light [7-9]. ZnO with a wideband gap (E_g= 3.37 eV) is one of the most important photocatalysts, which has been widely used in photocatalytic degradation of organic pollutants [10–12]. However, for the actual applications, traditional ZnO photocatalysts are usually not suitable due to the inconvenient and expensive separation [13], high photocorrosion [14], and low quantum efficiency resulted from its wide band gap and the rapid recombination of photo-generated carriers [15]. Therefore, it is a great challenge to make ZnO-based photocatalysis active under visible light. In this regard, the modified ZnO-based photocatalysis with conducting polymers such as PANI can respond to visible light region effectively [16-18]. PANI

has shown high absorption coefficient in the visible light range and high mobility of charge carriers. Under the irradiation of visible light, PANI not only is an electron donor but also itself is an excellent hole acceptor [19–21]. Moreover, from the practical view the ZnO-based photocatalysis coupled with conducting polymers are difficult to separate and recover from aqueous solution. However, the magnetic component used is often unstable in acidic medium and may interact with substrates. In this regard, $MnFe_2O_4$ as the important magnetic materials have been utilized with photocatalysts and allowing easy separation of the photocatalysts from the liquid after the photocatalytic process [22,23]. In this study, we provide a simple method to synthesize the magnetically recyclable PANI/$MnFe_2O_4$/ZnO photocatalyst by in situ oxidative polymerization method. Moreover, under visible light irradiation both of pure $MnFe_2O_4$ and PANI exhibit poor photocatalytic activity and pure ZnO shows a little higher photocatalytic activity. However, when PANI was combined with $MnFe_2O_4$ and PANI, the resulting compound show an enhanced photocatalytic activity for degradation of Methyl orange (MO) under visible light. Also, the stability and reusability of PANI/$MnFe_2O_4$/ZnO photocatalyst was also examined. This study could greatly promote the potential applications of magnetic ZnO-based photocatalysts in eliminating hazardous contaminants.

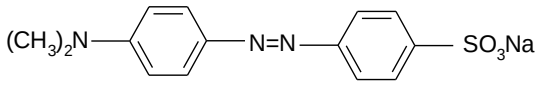

Figure 1: The chemical structure of Methyl orange

2. Experimental

2.1. Materials

Methyl orange, aniline, nitric acid, ammonium peroxydisulfate, $Fe(NO_3)_3.9H_2O$, $Mn(NO_3)_2.4H_2O$, ZnO and NaOH were purchased from Merck Company.

2.2. Instrumentation

The prepared samples were characterized by using XRD (Holland Philips Xpert, X-ray diffractometer with Cu-Kα radiation), field emission scanning electron microscopy and energy dispersive X-ray spectroscopy (FE-SEM, EDX, Vega 2 Tscan), a Fourier transform infrared spectrometer (JASCO FTIR-4200) and UV–Vis spectrophotometer (Shimadzu-2550).

2.3. Synthesis of $MnFe_2O_4$

For preparation of the $MnFe_2O_4$, 4.4 g $Fe(NO_3)_3.9H_2O$ and0.89 g $Mn(NO_3)_2.4H_2O$ were dissolved in 50 mL EtOH solution. Then 15 mL of the NaOH 4M solution was added dropwise into the above solution. After stirring the mixture for 3 h at 30 °C, the product was separated, washed with distilled water several times and dried at 60 °C. Then heat treatment of the product was carried out at 900 °C for 2 h.

2.4. Synthesis of PANI/$MnFe_2O_4$/ZnO photocatalyst

The PANI/$MnFe_2O_4$/ZnO sample was prepared byin situ polymerization of aniline on the surface of the $MnFe_2O_4$and ZnO samples that reported previously [24]. In this procedure, 10 mL of 0.1 M aniline, 10 mL of 0.125 ammonium peroxydisulfate and 30 mL of 0.1 M nitric acid solutions were added to 0.1g of synthesized $MnFe_2O_4$ and 0.25g of ZnO at room temperature. Then, the mixture was stirred during the polymerization of aniline, which was completed within 24 h. Finally, the prepared sample PANI/$MnFe_2O_4$/ZnO was dried at 60°C.

2.5. The photocatalytic experiments

In this study the dye MO solution was chosen as an environmental pollutant model. The disappearance of the peaks at λ_{max} = 466 nm was chosen for monitoring of dye decolorization for MO solution. In each experiment, 0.10 g of the PANI/$MnFe_2O_4$/ZnO as photocatalyst was added in 100 mL to the above solution with a V/V ration of 1:1. Air was blown into the reaction vessel by an aquarium pump to maintain the solution saturated with oxygen. In this research, a 100W filament tungsten lamp was used as the visible light source. The degree of photodecolorization(X), as a function of time, is given by Eq. (1)

$$X = \frac{C_0 - C_t}{C_0} \times 100 \quad (1)$$

Where C_0 is the initial concentration of dye, and C_t is the concentration of dye at time t. The progress of photocatalytic decolorization was measured by UV–Vis spectrophotometer (Shimadzu UV-2550).

3. Results and Discussion

3.1. Characterization of PANI/$MnFe_2O_4$/ZnO

The Fourier transform infrared (FT-IR) spectra of the as-synthesized PANI/$MnFe_2O_4$/ZnO sample in Fig.2 demonstrated two peaks at 3404 and 1631 cm^{-1} that are attributed to the absorbed water molecules on the surface of the sample. Also, the two peaks at 560 and 425 cm^{-1} are attributed to the vibrations of Zn-O and Fe-O bonds, respectively [25].

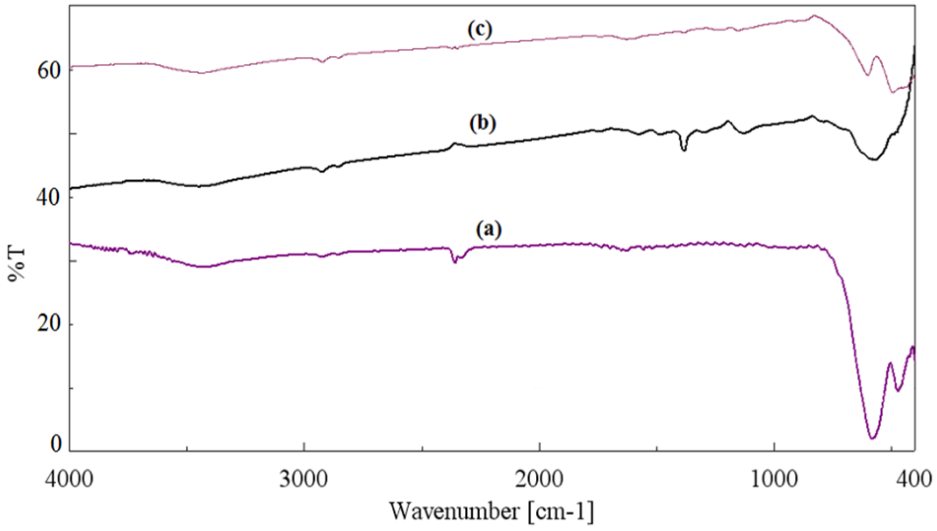

Figure 2: FT-IR spectrum of (a) $MnFe_2O_4$, (b) PANI/$MnFe_2O_4$ and (c)PANI/$MnFe_2O_4$/ZnO

The XRD patterns of ZnO, $MnFe_2O_4$ and PANI/$MnFe_2O_4$/ZnO are shown in Fig.3. The XRD patterns of ZnO and $MnFe_2O_4$ are in accordance with reported literature [26, 27]. The magnetic sample of PANI/$MnFe_2O_4$/ZnO shows the characteristic peaks of both ZnO and $MnFe_2O_4$. However, it could be noticed that the characteristic diffraction peak of $MnFe_2O_4$ in the PANI/$MnFe_2O_4$/ZnO was weak, which could be attributed to the low amount of the $MnFe_2O_4$ used in the synthesis of PANI/$MnFe_2O_4$/ZnO. The peaks corresponding to polyaniline are not detected, indicating that polyaniline was amorphous in the synthesized PANI/$MnFe_2O_4$/ZnO. No peak for another crystal phase is detected, indicating that there is no crystal phase impurity in the obtained sample.

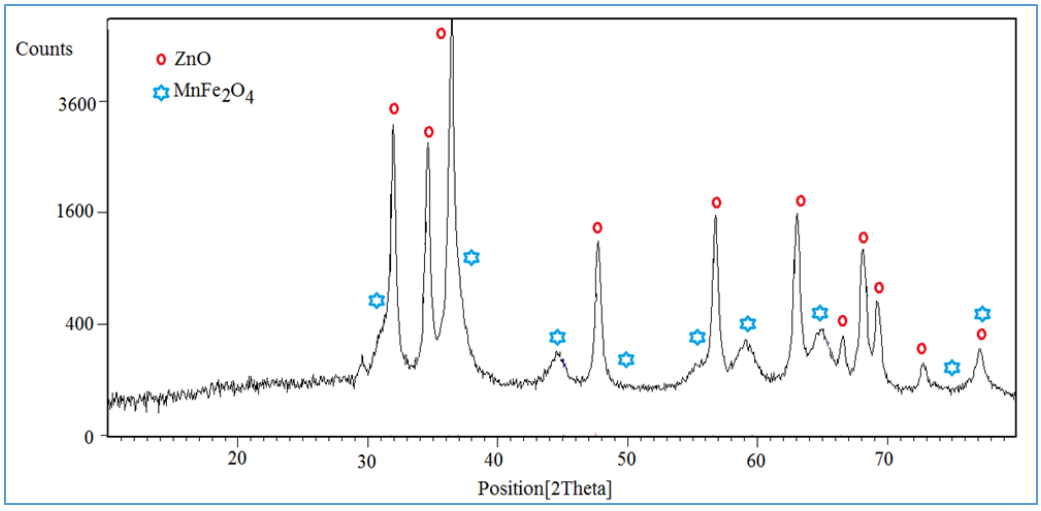

Figure 3: XRD curve of PANI/$MnFe_2O_4$/ZnO

The morphologies of $MnFe_2O_4$, and PANI/$MnFe_2O_4$/ZnO were studied by SEM. The SEM images of the PANI/$MnFe_2O_4$/ZnO sample are shown in Fig.4. Comparing the morphology of PANI/$MnFe_2O_4$/ZnO with that of $MnFe_2O_4$, it clearly suggests that the introduction of PANI and $MnFe_2O_4$is of great importance for obtaining a novel material. As expected, the microspheres of PANI are uniformly spherical which can be seen from SEM images of the PANI/$MnFe_2O_4$/ZnO sample.

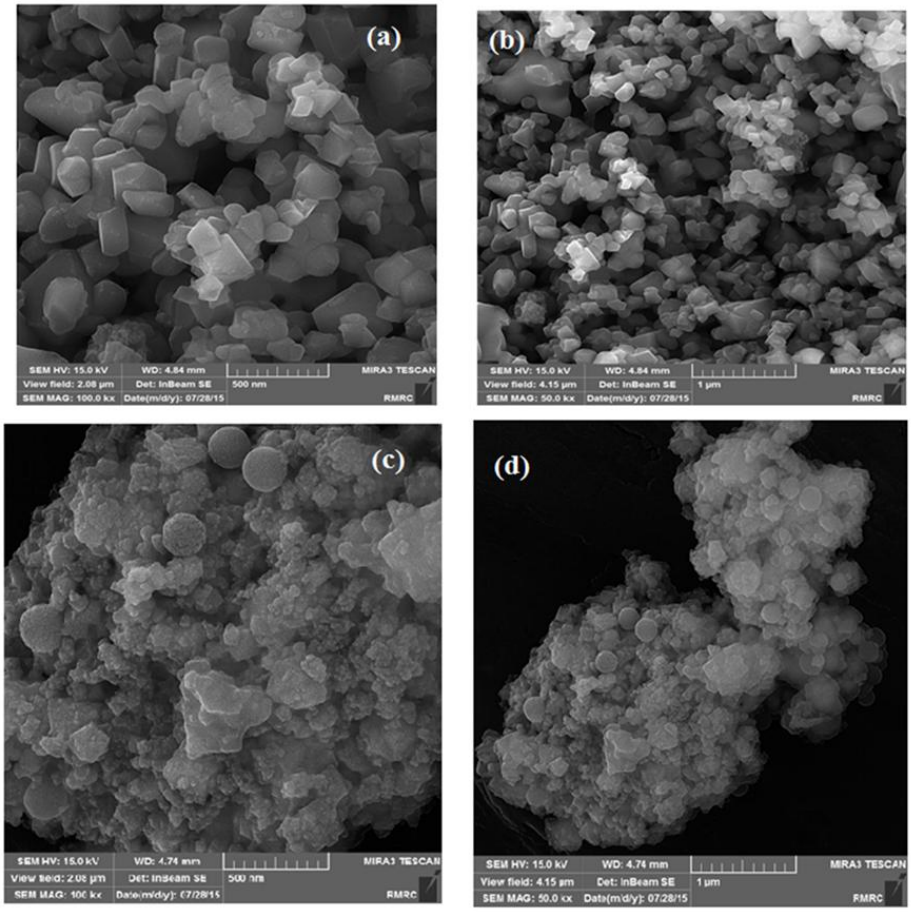

Figure 4: SEM images of pure $MnFe_2O_4$ (a)& (b)PANI/$MnFe_2O_4$/ZnO (c) & (d)

3.2. Photocatalytic degradation of MO over $MnFe_2O_4$, PANI/$MnFe_2O_4$ and PANI/$MnFe_2O_4$/ZnO samples

To evaluate activity of the prepared PANI/$MnFe_2O_4$/ZnO, the degradation of MO under visible light irradiation was considered. When photocatalyst absorbs visible radiation, it will produce pair of electrons and holes. These charge carriers can recombine, or the holescan be scavenged by oxidizing species and electrons by reducible species in the solution, which finally, lead to the destruction of many organic pollutants. The radicals are formed by scavenging of electrons and holes via molecular oxygen and water [28]. The active species generated by photo-irradiation will attack the pollutant, if this is in the very close vicinity of the photocatalyst. Generally, the photocatalytic kinetic of dye solution can be described by the Eq. (2) [29].

$$\ln (C_0/C_t) = k_{app}\, t \qquad (2)$$

Where C_0 is the concentrations of dye solution, C_t is the concentration ofdye solution at time t and k_{app} is the apparent rate constant. Generally, linear correlation of $\ln(C_0/C_t)$ versus time plot suggests a pseudo first order reaction. The plot of $\ln(C_0/C_t)$ versus time for the PANI/$MnFe_2O_4$/ZnO, PANI/$MnFe_2O_4$ and $MnFe_2O_4$ samples were presented in Fig. 6. The rate constant for the PANI/$MnFe_2O_4$/ZnO,PANI/$MnFe_2O_4$ and $MnFe_2O_4$ samples was obtained as 0.012, 0.006 and 0.0055 min^{-1}, respectively.

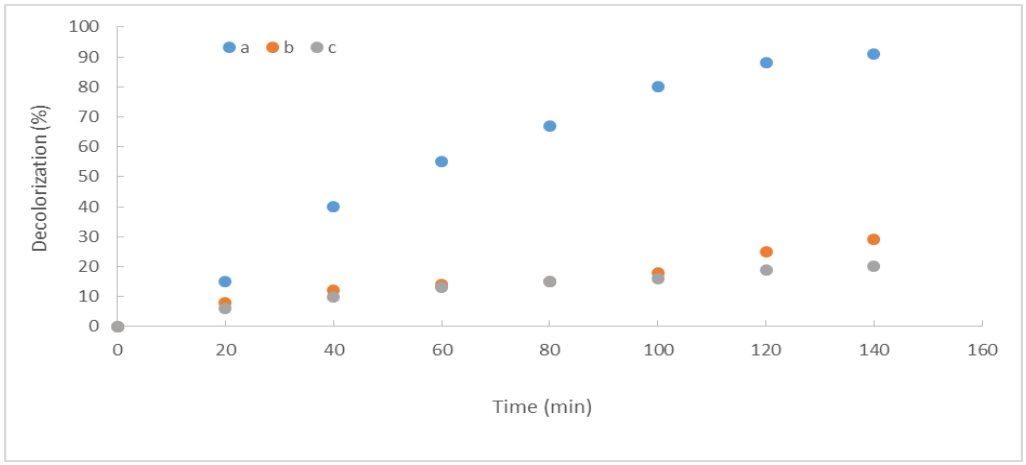

Figure 5: Photodecolorization of MO as a function of the irradiation time for (a) $MnFe_2O_4$, (b) PANI/$MnFe_2O_4$ and (c) PANI/$MnFe_2O_4$/ZnO

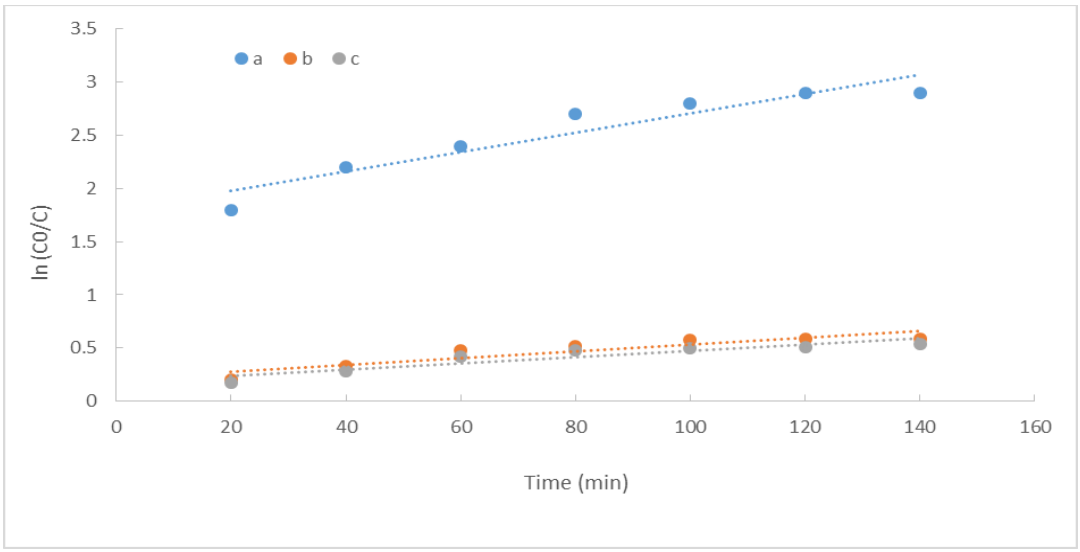

Figure 6: Photocatalytic kinetic of MO solutionfor (a) $MnFe_2O_4$,(b) PANI/$MnFe_2O_4$ and (c) PANI/$MnFe_2O_4$/ZnO

3.3. Mechanism of photocatalytic activity

The mechanism of photocatalytic MO degradation over PANI/$MnFe_2O_4$/ZnO under visible light is presented in Fig. 6. When irradiated under visible light, PANI can absorb visible light to induce the transitions π→ polaron and polaron→ π*, delivering the excited-state electrons of the highest unoccupied molecular orbital (HOMO) to the lowest unoccupied molecular orbital (LUMO). On the basis of the synergistic effect, the excited-state electrons in the LUMO of PANI molecules can migrate into the CB of ZnO subsequently, they transfer to the surface of ZnO and react with water to produce superoxide radical, which could oxidize the organic molecules. As a photosensitizer, PANI makes wonderful contributions to the still highly photocatalytic activity under visible light which attribute to that hydroxyl radicals and superoxide anions were produced by them, and the most important is that•OH would oxidize the organic dyes [30].

4. Conclusion

In summary, PANI/$MnFe_2O_4$/ZnO photocatalyst are prepared by in situ oxidative polymerization of aniline in the presence of $MnFe_2O_4$ and ZnO and for the first time which has enhanced photocatalytic activity under visible light irradiation and can be separated using an external magnet. The photocatalytic degradation experiments demonstrate

that the as-prepared catalyst displayed a high photocatalytic activity toward MO under visible light irradiation with their own optimum experimental condition.

Acknowledgements
We are grateful to Payame Noor University for its financial support.

References

1. Height, M. J., Pratsinis, S. E., Mekasuwandumrong, O., & Praserthdam, V. (2006). Ag-ZnO catalysts for UV-photodegradation of methylene blue. *Applied Catalysis B: Environmental*, 63(3): 305–312.
2. Tanaka, K., Padermpole, K., & Hisanaga, T. (2000). Photocatalytic degradation of commercial azo dyes. *Water Research*, 34(1): 327–333.
3. Zhong, D.K., Sun, J.W., Inumaru, H., & Gamelin, D.R. (2009). Solar water oxidation by composite catalyst/α-Fe_2O_3 photoanodes. *Journal of the American Chemical Society*, 131(17): 6086–6087.
4. Zhong, D.K., & amelin, D.R. (2010). Photoelectrochemical water oxidation by cobalt catalyst (''Co–Pi'')/α-Fe_2O_3 composite photoanodes: oxygen evolution and resolution of a kinetic bottleneck. *Journal of the American Chemical Society*, 132: 4202–4207.
5. Gonzalez-Valls, I., & Lira-Cantu, M. (2009). Vertically-aligned nanostructures of ZnO for excitonic solar cells: a review. *Energy & Environmental Science*, 2 (1): 19–34.
6. Kaneco, S., Katsumata, H., Suzuki, T., & Ohta, K. (2006). Titanium dioxide mediated photocatalytic degradation of dibutylphthalate in aqueous solution–kinetics, mineralization and reaction mechanism. *Chemical Engineering Journal*, 195: 59–66.
7. Wang, L., Wei, H., Fan, Y., Gu, X., & Zhan, J. (2009). One-dimensional CdS/α-Fe_2O_3 and CdS/Fe_3O_4 heterostructures: epitaxial and nonepitaxial growth and photocatalytic activity. *Journal of Physical Chemistry C*, 113 (32): 14119–14125.
8. Bandara, J., Mielczarski, J.A., & Kiwi, J. (1999). Molecular mechanism of surface recognition. Azo dyes degradation on Fe, Ti, and Al oxides through metal sulfonate complexes. *Langmuir*, 15 (22): 7670–7679.
9. Feng, J., Hu, X., & Yue, P.L. (2004). Discoloration and mineralization of orange II using different heterogeneous catalysts containing Fe: a comparative study. *Environmental Science & Technology*. 38 (21): 5773–5778.
10. Chattopadhyay, K.K., Maiti, S., &Pal, S. (2015). Recent advances in low temperature, solution processed morphology tailored ZnO nano-architecture for electronemission and photocatalysis applications. *Cryst Eng Comm*, 17 (48): 9264–9295.
11. Chen, Y., Zhang, C., Huang, W., Situ, Y., & Huang, H. (2015). Multimorphologies nano-ZnO preparing through a simple solvothermal method for photocatalytic application. *Materials Letters*, 141: 294–297.
12. Colmenares, J.C., Kuna, E., Jakubiak, S., Michalski, J., & Kurzydłowski, K. (2015). Polypropylene nonwoven filter with nanosized ZnO rods: promising hybrid photocatalyst for water purification. *Applied Catalysis B: Environmental*, 170–171: 273–282.
13. Li, Y., Wang, K., Wu, J., Gu, L., Lu, Z., Wang, X., & Cao, X. (2015). Synthesis of highly permeable Fe_2O_3/ZnO hollow spheres for printable photocatalysis.*RSC Advances.* 5: 88277–88286.
14. Han, C., Yang, M.Q., Weng, B., &Xu, Y.J. (2014). Improving the photocatalytic activity and anti-photocorrosion of semiconductor ZnO by coupling with versatile carbon. *Physical Chemistry Chemical Physics.* 16: 16891–16903.
15. Tang, D., Ye, H., Du, D., Liu, S., Li, M., Wu, X., Wen, L., Lv, K., & Deng, K. (2015). Fabrication of ZnO/graphene flake-like photocatalyst with enhanced photoreactivity. *Applied Surface Science*. 358: 130–136.

16. Eskizeybek, V., Sarı, F., Gülce, H., Gülce, A., & Avcı. A. (2012). Preparation of the New Polyaniline/ZnO Nanocomposite and its Photocatalytic Activity for Degradation of Methylene Blue and Malachite Green Dyes Under UV and Natural Sunlight Irradiations. *Applied Catalysis B: Environmental*, 119: 197–206.
17. Li, J., Xiao, Q., Li, L., Shen, J., & Hu. D. (2015). Novel ternary composites: Preparation, performance and application of $ZnFe_2O_4/TiO_2$/polyaniline. *Applied Surface Science*, 331: 108–114.
18. Xiong, P., Wang, L., Sun, X., Xu, B., & Wang. X. (2013).Ternary Titania–Cobalt Ferrite–Polyaniline Nanocomposite: A Magnetically Recyclable Hybrid for Adsorption and Photodegradation of Dyes under Visible Light. *Industrial & Engineering Chemistry Research*, 52 (30): 10105–10113
19. Shaheen, S.E.,Brabec, C.J., Sariciftci, N.S., Padinger, F., Fromherz, T., & Hummelen. J.C. (2001). 2.5% efficient organic plastic solar cells. *Applied Physics Letters*. 78: 841–843.
20. Lin, Y.M., Li, D.Z., Hu, J.H., Xiao, G.C., Wang, J.X. Li, W.J., & Fu, X.Z. (2012). Highly efficient photocatalytic degradation of organic pollutants by PANI-modified TiO_2composite. *Journal of Physical Chemistry C* 116 (9): 5764–5772.
21. Shirota, Y., & Kageyama, H. (2007). Charge carrier transporting molecular materials and their applications in devices. *Chemical Reviews.* 107 (4): 953–1010.
22. Sun, S.H., Zeng, H., Robinson, D.B., Raoux, S., Rice, P.M., Wang, S.X., & Li, G.X. (2004). Mono disperse MFe_2O_4 (M = Fe, Co, Mn) nanoparticles. *Journal of the American Chemical Society*. 126 (1):273–279.
23. Chen, Q., Qinqin, H., Mengmeng, L., Xueting, L., Wang, J., & Lv, J. (2014). The vital role of PANI for the enhanced photocatalytic activity of magnetically recyclable N–$K_2Ti_4O_9/MnFe_2O_4$/PANI composites. *Applied Surface Science* 311: 230–238.
24. Li, X.Y., Wang, D.S., Cheng, G.X., Luo, Q.Z., An, J., & Wang, Y.H. (2008). Preparation of polyaniline-modified TiO_2 nanoparticles and their photocatalytic activity under visible light illumination. *Applied Catalysis B: Environmental*, 81: 267–273.
25. Dhiman, M., Sharma, R., Kumar, V., Singhal, S. (2016). Morphology controlled hydrothermal synthesis and photocatalytic properties of $ZnFe_2O_4$ nanostructures. *Ceramics International*, 42 (11): 12594–12605.
26. Allen, M.R., Thibert, A., Sabio, E.M., Browning, N.D., Larsen, D.S., & Osterloh, F.E. (2010). Evolution of physical and photocatalytic properties in the layered titanates $A_2Ti_4O_9$ (A = K, H) and in nanosheets derived by chemical exfoliation. *Chemistry of Materials*. 22: 1220–1228.
27. Winiarska, K., Szczygieł, I., & Klimkiewicz, R. (2013). Manganese-Zinc ferrite synthesis bythe sol-gel autocombustion method, effect of the precursor on the ferrite'scatalytic properties. *Industrial & Engineering Chemistry Research.* 52: 353–361.
28. Casbeer, E., Sharma, V.K., &Li, X. Z. (2012). Synthesis and photocatalytic activity of ferrites under visible light: a review. *Separation and Purification Technology*. 87: 1–14.
29. Trandafilovic, L.V., Jovanovic, D.J., Zhang, X., Ptasinsk, S., & Dramicanin, M.D. (2017). Enhanced photocatalytic degradation of methylene blue and methyl orange by ZnO: Eu nanoparticles. *Applied Catalysis B: Environmental* 203: 740–752.
30. Zhang, X., Wu, J., Meng, G., Guoa, X., Liu, Ch., & Liu, Z. (2016). One-step synthesis of novel PANI–Fe_3O_4@ZnO core–shellmicrospheres: An efficient photocatalyst under visible light irradiation. *Applied Surface Science* 366: 486–493.